Accelerated Publications

Catalase Is Regulated by Ubiquitination and Proteosomal Degradation. Role of the c-Abl and Arg Tyrosine Kinases†

Cheng Cao,‡,§ Yumei Leng,§ Xuan Liu,‡ Yanping Yi,‡ Ping Li,‡ and Donald Kufe*,§

Beijing Institute of Biotechnology, Beijing 100850, Peoples Republic of China, and Dana-Farber Cancer Institute, Harvard Medical School, Boston, Massachusetts 02115

Received June 16, 2003; Revised Manuscript Received August 4, 2003

ABSTRACT: Catalase is a major effector in the defense of aerobic cells against oxidative stress. Recent studies have shown that catalase activity is stimulated by the c-Abl and Arg tyrosine kinases. Little, however, is otherwise known about the mechanisms responsible for catalase regulation. The present work demonstrates that mouse cells deficient in both c-Abl and Arg exhibit increased catalase stability. The results also show that catalase is subject to ubiquitination and degradation by the 26S proteosome. Significantly, ubiquitination of catalase is dependent on c-Abl- and Arg-mediated phosphorylation of catalase on both Y231 and Y386. In concert with these results, human 293 cells expressing catalase mutated at Y231 and Y386 exhibit attenuated levels of reactive oxygen species when exposed to hydrogen peroxide. These findings indicate that, in addition to stimulating catalase activity, c-Abl and Arg promote catalase degradation in the oxidative stress response.

Normal aerobic metabolism is associated with the production of reactive oxygen species (ROS)[1] and, as a result, damage to DNA, proteins, and lipids (*1*, *2*). ROS production has also been associated with the induction of apoptosis (*3*, *4*). Studies have demonstrated that ROS-induced apoptosis is p53-dependent (*5*, *6*). Other work has shown that the $p66^{shc}$ adaptor protein (*6*), the p85 subunit of phosphatidylinositol 3-kinase (*5*), and topoisomerase II are involved in the apoptotic response to oxidative stress.

The ubiquitously expressed c-Abl nonreceptor tyrosine kinase and the product of the *c-abl*-related gene (Arg) (*7*) have been implicated in the cellular responses to oxidative and other types of stress (*8*−*11*). Cytoplasmic c-Abl is activated in cells exposed to hydrogen peroxide (H_2O_2) by a mechanism dependent on protein kinase Cδ (*9*, *12*). Activation of c-Abl in response to oxidative stress is associated with targeting of c-Abl to mitochondria, loss of mitochondrial transmembrane potential, and release of cytochrome *c* (*12*, *13*). Consistent with these findings, cells deficient in c-Abl exhibit resistance to H_2O_2-induced apoptosis and necrosis (*12*, *13*). Other studies have demonstrated that Arg is activated by oxidative stress and that H_2O_2-induced apoptosis is attenuated in Arg-deficient cells (*10*). Moreover, the available findings indicate that ROS induce c-Abl−Arg heterodimers and that both c-Abl and Arg are necessary as effectors in the apoptotic response to oxidative stress (*14*).

Catalase regulates intracellular ROS levels by converting H_2O_2 to H_2O and O_2 in peroxisomes (*15*). However, the mechanisms responsible for the regulation of catalase are largely unknown. Recent studies have shown that c-Abl and Arg phosphorylate catalase and thereby stimulate catalase activity (*16*). The present studies demonstrate that c-Abl and Arg also target catalase for destruction by the 26S proteosome. The results show that catalase is subject to ubiquitination by a mechanism dependent on c-Abl- and Arg-mediated phosphorylation.

EXPERIMENTAL PROCEDURES

Cell Culture. Wild-type mouse embryo fibroblasts, *c-abl*$^{-/-}$, *arg*$^{-/-}$, *c-abl*$^{-/-}$*arg*$^{-/-}$ (*17*), and 293 cells were grown in Dulbecco's modified Eagle's medium (DMEM) supplemented with 10% heat-inactivated fetal bovine serum (HI-FBS), 2 mM L-glutamine, 100 units/mL penicllin, and 100 μg/mL streptomycin. Cells were treated with cycloheximide (Sigma), lactacystin (Calbiochem), MG132 (Peptide Institute, Inc.), or L-buthionine sulfoxime (BSO; Sigma).

Immunoprecipitation and Immunoblot Analysis. Cell lysates were prepared in lysis buffer (50 mM Tris-HCl, pH 7.5, 1 mM phenylmethanesulfonyl fluoride, 1 mM dithiothreitol, 10 mM sodium fluoride, and 10 μg/mL aprotinin, leupeptin, and pepstatin A). Proteins were subjected to immunoblot analysis with anti-catalase (Calbiochem), anti-β-actin (Sigma), anti-Arg (*10*), anti-ubiquitin (Santa Cruz Biotechnology), anti-Flag (M5, Sigma), anti-green fluores-

† This investigation was supported by Grants CA42802 and CA98628 awarded by the National Cancer Institute and Grant 30270316 awarded by the National Science Foundation of China.

* To whom correspondence should be addressed. Phone: (617) 632-3141. Fax: (617) 632-2934. E-mail: Donald_Kufe@dfci.harvard.edu.

‡ Beijing Institute of Biotechnology.

§ Harvard Medical School.

[1] Abbreviations: ROS, reactive oxygen species; Arg, product of the *c-abl*-related gene; H_2O_2, hydrogen peroxide; BSO, L-buthionine sulfoxime; GFP, gene fluorescence protein; Ub, ubiquitin.

10.1021/bi035023f CCC: $25.00
Published on Web 08/15/2003

cence protein (GFP; Clontech), anti-Myc (Santa Cruz Biotechnology), or anti-P-Tyr (4G10; Upstate Biotechnology). Soluble proteins were also subjected to immunoprecipitation with anti-catalase (Sigma), anti-ubiquitin, anti-Myc, or anti-Flag, and the resulting immunoprecipitates were analyzed by immunoblotting. The antigen−antibody complexes were visualized by chemiluminescence (ECL; Amersham Pharmacia Biotech).

Vectors. Calatase cDNA sequences were amplified from a HeLa cell library (Clontech) by polymerase chain reactions. Flag-tagged human catalase (*16*) and catalase mutants were constructed by cloning into the pcDNA3.1-based Flag vector. All mutations were confirmed by DNA sequencing. pEGFP (Clontech) and the other vectors were transfected into cells in the presence of Lipofectamine (Life Technologies, Inc). Cells were transduced with a retrovirus expressing Arg (*17*).

Pulse−Chase Experiments. 293 cells were transfected with Flag-catalase, incubated for 18 h, and washed with methionine-free DMEM. The cells were then incubated with methionine-free DMEM containing 10 μCi/mL [^{35}S]methionine (New England Nuclear) for 45 min, washed, cultured in complete DMEM containing 10% HI-FBS, and harvested at the indicated times. Immunoprecipitates were subjected to SDS−PAGE and autoradiography.

In Vitro Degradation Assays. Flag-catalase DNAs were incubated in the TNT T7 Quick coupled transcription/translation system (Promega) supplemented with 0.4 μCi/μL [^{35}S]methionine for 1 h. The ^{35}S-labeled Flag-catalase protein was incubated in degradation mix (33% rabbit reticulocyte lysate, 50 mM Tris-HCl, pH 8.0, 5 mM $MgCl_2$, 2 mM dithiothreitol, 1 mM ATP, and 2 mM methionine) at 37 °C for the indicated times. In certain experiments, ATP was substituted with 2 mM ATPγS (Calbiochem). The ^{35}S-labeled proteins were analyzed by SDS−PAGE and autoradiography.

Measurement of Intracellular ROS Levels. Cells were treated with 0.3 mM BSO (Sigma) for 16 h and then incubated with 5 μM DCF-DA (Sigma) for 30 min at 37 °C in the dark. The cells were then incubated in the absence and presence of 0.5 mM H_2O_2 for 30 min at 37 °C. Fluorescence of oxidized DCF was measured at an excitation wavelength of 480 nm and an emission wavelength of 525 nm by flow cytometry (Becton Dickinson). The geometric mean obtained from 10^4 cells was used to calculate the relative H_2O_2 concentration.

RESULTS

c-Abl and Arg Regulate Catalase Expression. To determine whether c-Abl or Arg regulates catalase expression, lysates from wild-type, *c-abl*$^{-/-}$, and *arg*$^{-/-}$ cells were analyzed by immunoblotting with anti-catalase. The results demonstrate little, if any, effect of c-Abl or Arg deficiency on catalase levels (Figure 1A, left). By contrast, catalase expression was increased 2.8−3-fold in *c-abl*$^{-/-}$*arg*$^{-/-}$ cells (Figure 1A, left). Similar results obtained in two separate clones of *c-abl*$^{-/-}$*arg*$^{-/-}$ cells indicated that the increase in catalase expression is not due to clonal variation (Figure 1A, left). Moreover, the finding by Northern analysis that catalase mRNA levels are similar in wild-type and *c-abl*$^{-/-}$*arg*$^{-/-}$ cells supported the involvement of a posttranscriptional mechanism (data not shown). To confirm that the absence of Arg is associated with increases in catalase, the *c-abl*$^{-/-}$*arg*$^{-/-}$ cells were transduced with a retrovirus expressing Arg (Figure 1A, right). Compared to *c-abl*$^{-/-}$*arg*$^{-/-}$ cells expressing the empty vector, Arg expression was associated with decreased levels of catalase (Figure 1A,

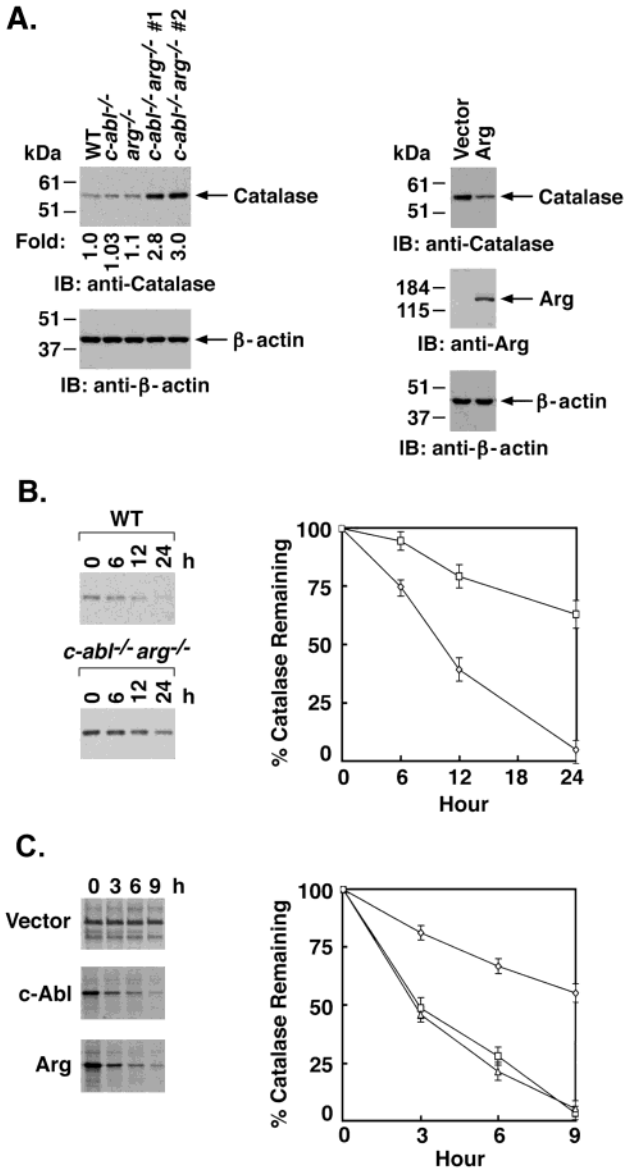

FIGURE 1: Catalase expression is regulated by c-Abl and Arg. (A) Lysates from wild-type (WT), *c-abl*$^{-/-}$, *arg*$^{-/-}$, and *c-abl*$^{-/-}$*arg*$^{-/-}$ (clones 1 and 2) cells were analyzed by immunoblotting with anti-catalase and anti-β-actin (left panel). *c-abl*$^{-/-}$*arg*$^{-/-}$ cells were infected with retroviruses expressing an empty vector or Arg. At 24 h after infection, lysates were analyzed by immunoblotting with anti-catalase, anti-Arg, and anti-β-actin (right panel). (B) Wild-type (WT) (◇) and *c-abl*$^{-/-}$*arg*$^{-/-}$ (□) cells were pulsed with [^{35}S]methionine, washed, and incubated for the indicated times. Anti-catalase immunoprecipitates were analyzed by SDS−PAGE and autoradiography (left panel). The intensity of the signals is presented as the percentage (mean ± SD of three experiments) of catalase remaining over time relative to control at 0 h (right panel). (C) 293 cells were cotransfected with Flag-catalase and the empty vector (◇), c-Abl (□), or Arg (△). At 24 h after transfection, the cells were pulsed with [^{35}S]methionine, washed, and incubated for the indicated times. Anti-Flag immunoprecipitates were analyzed by SDS−PAGE and autoradiography (left panel). The intensity of the signals is presented as the percentage (mean ± SD of three experiments) of catalase remaining over time relative to the control at 0 h (right panel).

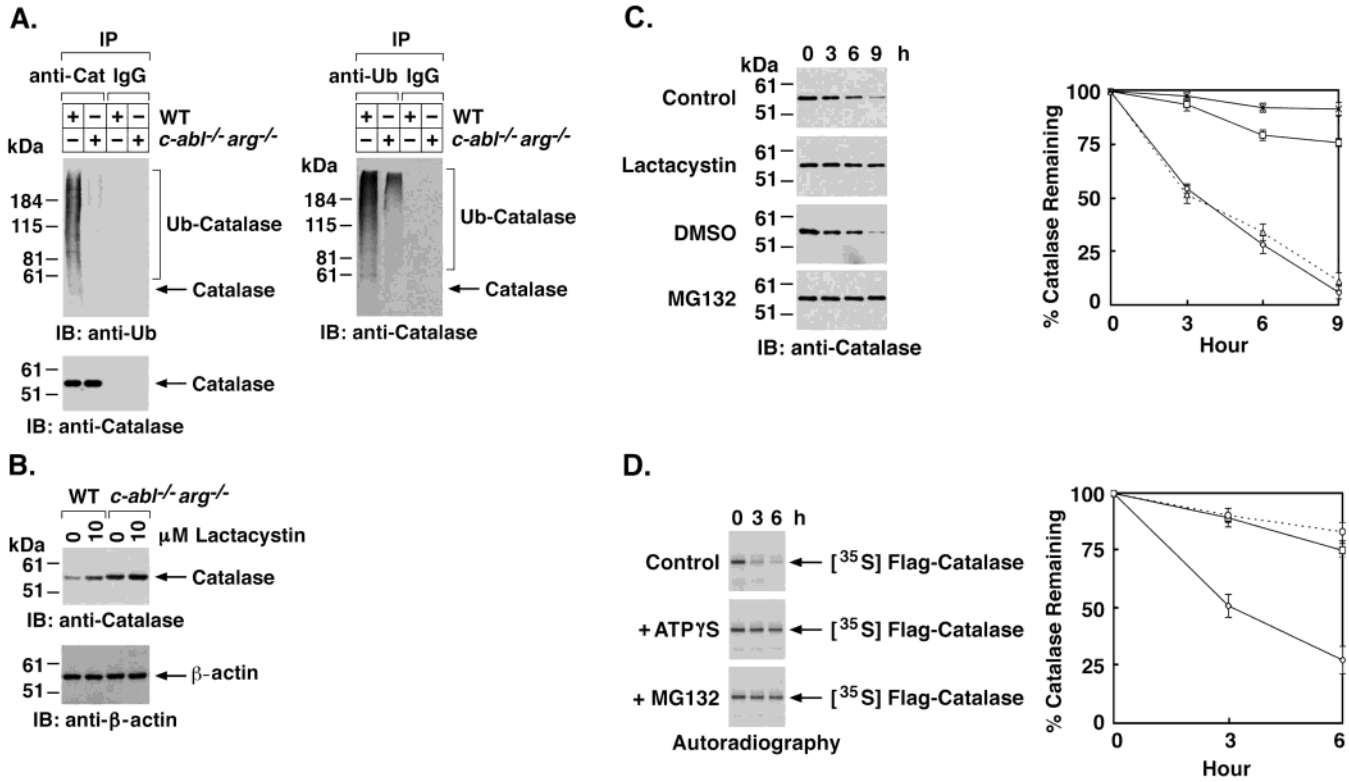

FIGURE 2: c-Abl and Arg regulate catalase stability and ubiquitination. (A) Wild-type and *c-abl*$^{-/-}$*arg*$^{-/-}$ cells were treated with 10 μg/mL MG132 for 4 h. Cell lysates were analyzed by immunoblotting with anti-catalase, normalized for catalase levels, and then subjected to immunoprecipitation with anti-catalase (left panel) or anti-Ub (right panel). Immunoprecipitations were performed with IgG as a control. The immunoprecipitates were analyzed by immunoblotting with anti-Ub or anti-catalase. (B) Wild-type and *c-abl*$^{-/-}$*arg*$^{-/-}$ cells were incubated in the absence and presence of 10 μM lactacystin for 8 h. Lysates were subjected to immunoblotting with anti-catalase and anti-β-actin. (C) 293 cells were cotransfected to express Flag-catalase and c-Abl. At 12 h after transfection, cells were treated with 50 μg/mL cycloheximide ($\diamond$) or cycloheximide with 10 μM lactacystin ($\square$), 10 μM MG132 ($\times$), or, as a control for MG132, DMSO ($\triangle$) for the indicated times. Lysates were analyzed by immunoblotting with anti-catalase (left panel). The intensity of the signals was determined by densitometric scanning. The results are presented as the percentage (mean $\pm$ SD of three experiments) of catalase remaining over time relative to control (right panel). (D) In vitro translated ^{35}S-labeled Flag-catalase was incubated in degradation mix for the indicated times ($\diamond$). Reactions were performed in which ATPγS was substituted for ATP ($\bigcirc$) or in the presence of 10 μM MG132 ($\square$). The degradation products were analyzed by SDS$-$PAGE and autoradiography (left panel). The intensity of the signals is presented as the percentage (mean $\pm$ SD of three experiments) of catalase remaining over time relative to control (right panel).

right). To assess the stability of catalase, wild-type and *c-abl*$^{-/-}$*arg*$^{-/-}$ cells were pulsed with [^{35}S]methionine for 30 min and then chased for 0, 6, 12, and 24 h. The results show that the stability of catalase is increased in *c-abl*$^{-/-}$*arg*$^{-/-}$, as compared to wild-type, cells (Figure 1B, left). Densitometric scanning of the signals obtained in three experiments demonstrated catalase half-lives of $\sim$10.5 h in wild-type and $>$24 h in *c-abl*$^{-/-}$*arg*$^{-/-}$ cells (Figure 1B, right). To confirm the effects of c-Abl and Arg on catalase stability, 293 cells were transfected to express Flag-catalase and c-Abl or Arg. Cotransfection of Flag-catalase and the empty vector resulted in a half-life of $>$9 h (Figure 1C). By contrast, the half-life of catalase was $\sim$3 h when coexpressed with c-Abl or Arg (Figure 1C). These results indicate that c-Abl or Arg regulates catalase stability.

Catalase Is Subject to Ubiquitination and Proteosomal Degradation. To determine if catalase stability is regulated by the ubiquitin (Ub)$-$proteosome pathway, anti-catalase immunoprecipitates from wild-type cells were analyzed by immunoblotting with anti-Ub. The results show anti-Ub reactivity over a range of different electrophoretic mobilities (Figure 2A, left). By contrast, similar studies in *c-abl*$^{-/-}$*arg*$^{-/-}$ cells demonstrated a substantial decrease in anti-Ub reactivity (Figure 2A, left). As a control, immunoprecipitation of catalase was comparable from the wild-type and *c-abl*$^{-/-}$*arg*$^{-/-}$ cells (Figure 2A, left). In the reciprocal experiment, immunoblot analysis of anti-Ub immunoprecipitates with anti-catalase demonstrated a higher level of ubiquitinated catalase in wild-type as compared to *c-abl*$^{-/-}$*arg*$^{-/-}$ cells (Figure 2A, right). To determine if catalase is subject to proteosomal degradation, studies were performed with the proteosomal inhibitor, lactacystin. Treatment of wild-type cells with lactacystin was associated with an increase in catalase levels (Figure 2B). Lactacystin treatment of *c-abl*$^{-/-}$*arg*$^{-/-}$ cells was also associated with an increase in catalase levels, but to a lesser extent (Figure 2B). Lactacystin increased the half-life of catalase in 293 cells expressing Flag-catalase and c-Abl (Figure 2C). MG132, another proteosome inhibitor, also increased the half-life of catalase in cells (Figure 2C). Similar results were obtained with lactacystin and MG132 when Flag-catalase was coexpressed with Arg (data not shown). In an in vitro Ub$-$proteosome system, ^{35}S-labeled Flag-catalase was degraded at a half-life of approximately 3 h (Figure 2D). As a control, degradation was inhibited when ATPγS was substituted for ATP to prevent ubiquitination (Figure 2D). Degradation of catalase was also blocked when MG132 was added to the reaction (Figure 2D). These findings indicate that catalase is targeted for degradation by

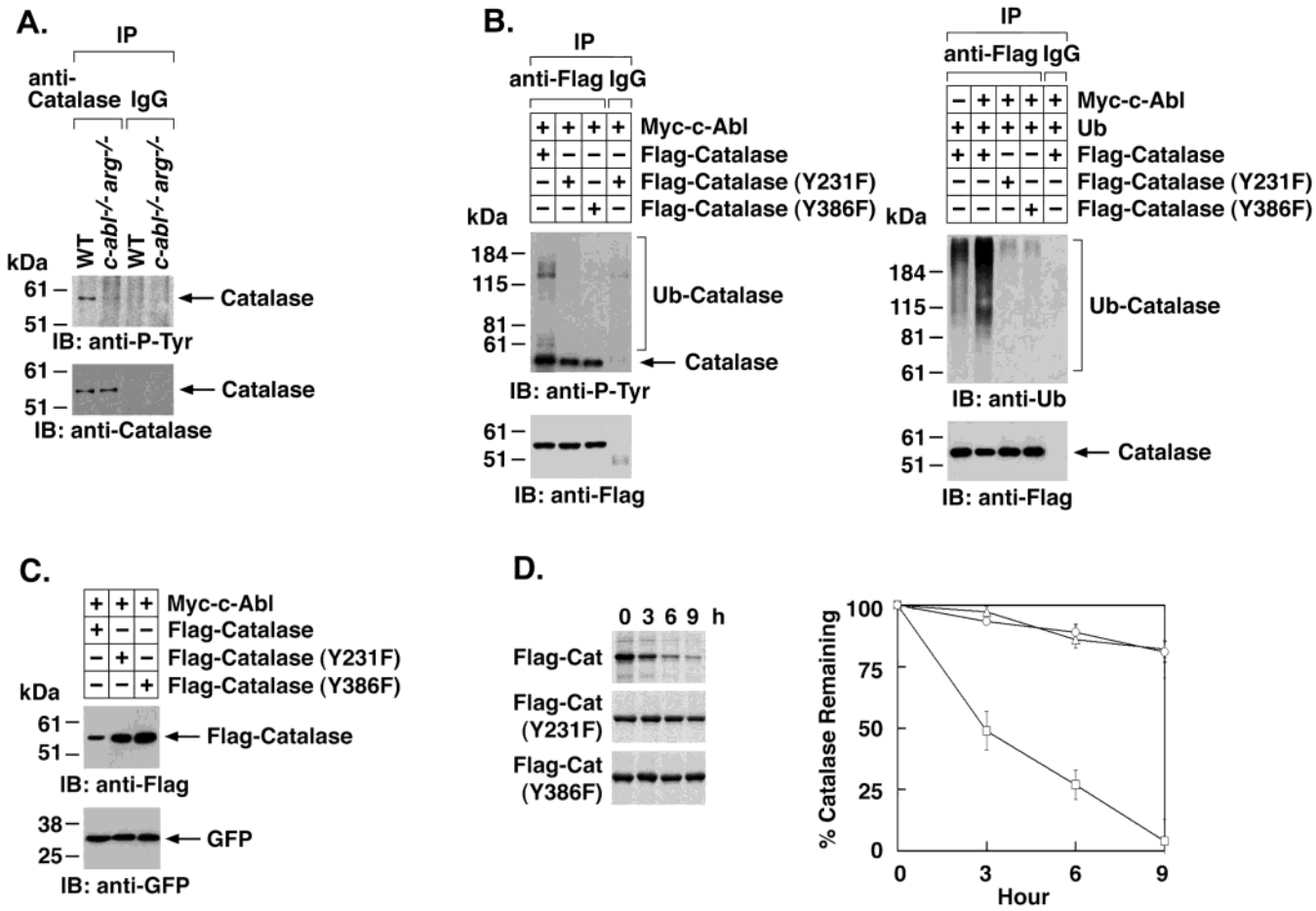

FIGURE 3: c-Abl-mediated phosphorylation regulates catalase ubiquitination and degradation. (A) Anti-catalase immunoprecipitates from wild-type and *c-abl*$^{-/-}$*arg*$^{-/-}$ cells were analyzed by immunoblotting with anti-P-Tyr. IgG immunoprecipitates were analyzed as controls. (B) Lysates from 293 cells expressing c-Abl and Flag-catalase or the indicated mutants were analyzed by immunoblotting with anti-catalase, normalized for the amount of catalase, and then subjected to immunoprecipitation with anti-Flag or IgG. The immunoprecipitates were analyzed by immunoblotting with anti-P-Tyr (left panel), anti-Ub (right panel), or anti-Flag. (C) 293 cells were transfected with Myc-c-Abl, GFP, and Flag-catalase or the indicated mutants. Lysates were analyzed by immunoblotting with anti-Flag and anti-GFP. (D) 293 cells expressing c-Abl and Flag-catalase (□), Flag-catalase(Y231F) (○), or Flag-catalase(Y386F) (△) were pulsed with [^{35}S]methionine and chased for the indicated times. Anti-Flag immunoprecipitates were analyzed by SDS−PAGE and autoradiography (left panel). The intensity of the signals is presented as the percentage (mean ± SD of three experiments) of catalase remaining over time relative to control (right panel).

the Ub−proteosome pathway and that this process is regulated by c-Abl and Arg.

Ubiquitination and Degradation of Catalase Are Regulated by c-Abl/Arg Phosphorylation. To assess tyrosine phosphorylation of endogenous catalase in vivo, anti-catalase immunoprecipitates from wild-type and *c-abl*$^{-/-}$*arg*$^{-/-}$ cells were analyzed by immunoblotting with anti-P-Tyr. The results demonstrate tyrosine phosphorylation of catalase in wild-type, but not *c-abl*$^{-/-}$*arg*$^{-/-}$, cells (Figure 3A). On the basis of the finding that catalase is phosphorylated on Y231 and Y386 by c-Abl and Arg (*16*), anti-Flag immunoprecipitates from cells expressing c-Abl and Flag-catalase mutated at Y231 or Y386 were analyzed for tyrosine phosphorylation and ubiquitination. Immunoblot analysis of anti-Flag immunoprecipitates with anti-P-Tyr demonstrated that c-Abl-mediated phosphorylation and ubiquitination of catalase are decreased by mutation of Y231 to F (Figure 3B, left). Decreases in tyrosine phosphorylation and ubiquitination were also observed with the catalase(Y386F) mutant (Figure 3B, left). Similar findings were obtained for Arg-mediated phosphorylation of wild-type catalase and the Y → F mutants (data not shown). Immunoblot analysis of the anti-Flag immunoprecipitates with anti-Ub confirmed that ubiquitination of catalase(Y231F) and catalase(Y386F) is substantially decreased compared to that of wild-type catalase (Figure 3B, right). Moreover, ubiquitination of wild-type Flag-catalase was increased by c-Abl, while c-Abl had little effect on ubiquitination of the catalase mutants (Figure 3B, right). In concert with these findings, expression of catalase(Y231F) and catalase(Y386F) was higher than that found for wild-type catalase (Figure 3C). In addition, the stability of catalase was increased by the Y231F or Y386F mutations (Figure 3D). Thus, the half-life of Flag-catalase was 3 h, while Flag-catalase(Y231F) and Flag-catalase(Y386F) had half-lives of >9 h (Figure 3D). These results demonstrate that tyrosine phosphorylation of catalase by c-Abl and Arg regulates catalase ubiquitination and degradation.

Intracellular ROS Levels Are Regulated by c-Abl/Arg-Mediated Catalase Degradation. To determine whether ROS levels are regulated by c-Abl/Arg-mediated catalase turnover, cells were treated with 0.5 mM H_2O_2 and monitored for oxidation of the fluorochrome DCF-DA. In this regard, treatment with >1.0 mM H_2O_2 decreases the interaction of catalase with c-Abl/Arg (*16*). Expression of c-Abl was

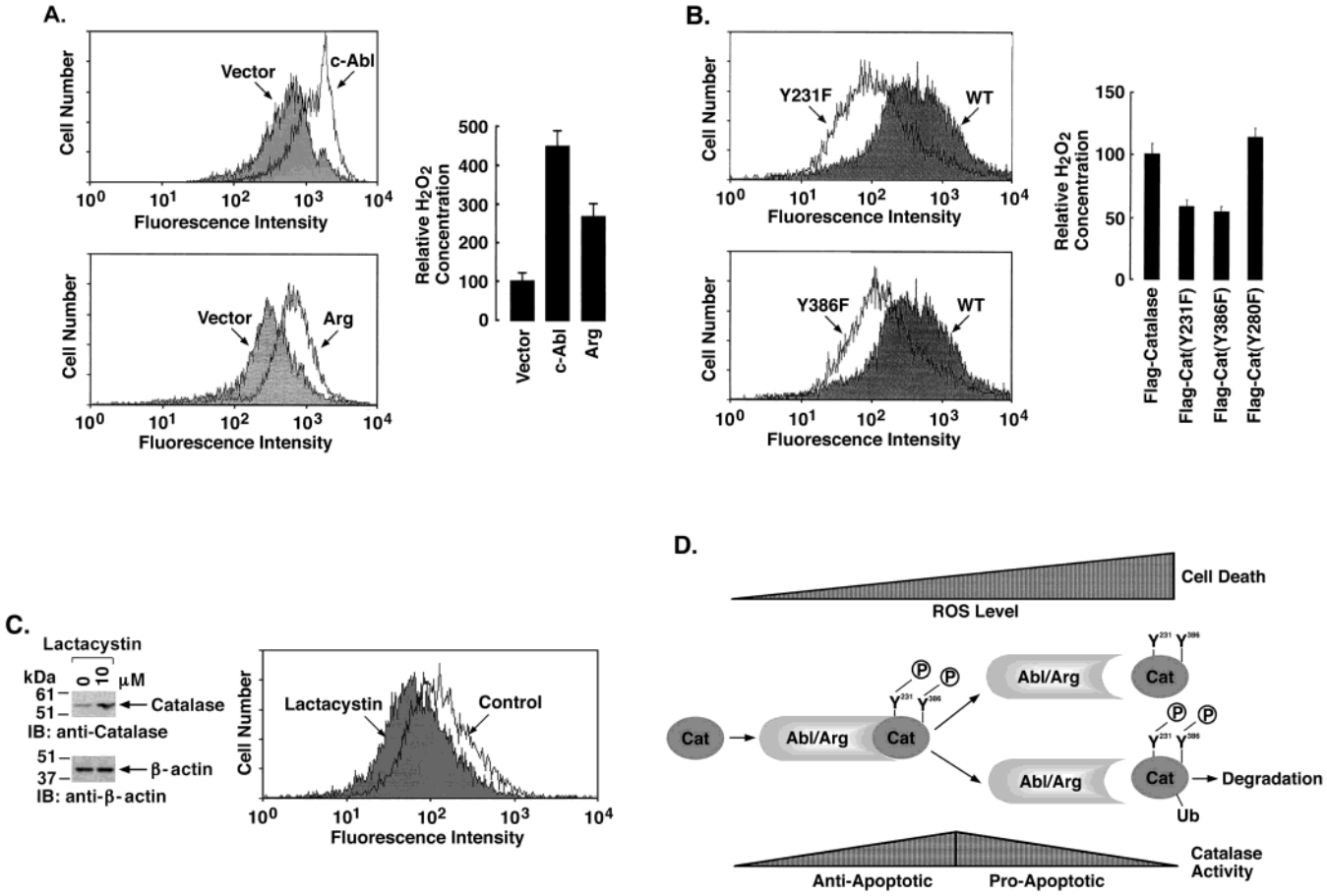

FIGURE 4: Intracellular oxidant levels are regulated by c-Abl/Arg-mediated catalase degradation. (A) 293 cells were transfected with 4 μg of vector, c-Abl, or Arg and 0.2 μg of pDSred. (B) 293 cells were transfected with 1 μg of Myc-c-Abl, 4 μg of Flag-catalase or the indicated mutants, and 0.2 μg of pDSred. At 12 h after transfection, cells were treated with 0.3 mM BSO for 16 h to inhibit glutathione peroxidase, incubated with DCF-DA, and then exposed to 0.5 mM H_2O_2 for 30 min. pRSred cells were analyzed by flow cytometry for oxidized DCF (left panel). The data (geometric mean $\pm$ SE for three experiments) are presented as the relative H_2O_2 concentration compared to that obtained for control cells (right panel). (C) Wild-type mouse fibroblasts were incubated in the absence and presence of 10 μM lactacystin for 4 h, and then 3 mM BSO was added to the medium for 8 h. The cells were stained with DCF-DA and then treated with 0.5 mM H_2O_2 for 30 min. Lysates were subjected to immunoblot analysis with anti-catalase and anti-β-actin (left panel). Cells were analyzed by flow cytometry for oxidized DCF (right panel). (D) Schematic representation of the proposed dual ROS-mediated anti-apoptotic and pro-apoptotic regulation of catalase by c-Abl and Arg.

associated with substantially higher ROS levels (Figure 4A). Similar findings were obtained in cells expressing Arg (Figure 4A). Intracellular ROS levels were also higher in cells expressing c-Abl and wild-type catalase but not catalase(Y231F) (Figure 4B). Moreover, ROS levels were attenuated in H_2O_2-treated cells expressing c-Abl and catalase(Y386F) (Figure 4B). As a control, expression of catalase mutated at Y280 had no effect on ROS levels (Figure 4B, right). To show that catalase turnover is relevant for its function in mediating oxidative stress, wild-type cells were treated with H_2O_2 in the presence and absence of lactacystin. The H_2O_2-induced decrease in catalase levels was attenuated by lactacystin (Figure 4C, left). Importantly, lactacystin treatment was also associated with lower intracellular ROS levels (Figure 4C, right). These findings collectively demonstrate that c-Abl/Arg-mediated phosphorylation of catalase regulates intracellular ROS levels.

DISCUSSION

Regulation of Catalase in the Response to Oxidative Stress. Aerobic cells require defense mechanisms against the substantial amount of oxygen that is reduced by the mitochondrial respiratory chain and converted to H_2O_2 (*18*). Surprisingly, little is known about how catalase, a major effector of that defense, is regulated in the response of cells to oxidative stress. The present findings provide new insights regarding the regulation of catalase. Our results show that c-Abl/Arg-mediated phosphorylation of catalase on both Y231 and Y386 is required for its ubiquitination and thereby degradation by the 26S proteosome (Figure 4D). On the basis of these findings, c-Abl- or Arg-mediated degradation of catalase would be predicted to abrogate this major defense against accumulation of H_2O_2 and amplify ROS-induced apoptosis and/or necrosis. Indeed, the present results show that expression of c-Abl or Arg is regulated by intracellular ROS levels. Moreover, expression of catalase with mutations at Y231 or Y386, but not wild-type catalase, attenuated the higher ROS levels associated with H_2O_2 exposure. Attenuation of H_2O_2-induced catalase turnover by inhibition of proteosomal degradation was also associated with lower ROS levels. These results collectively provide support for a model in which c-Abl- and/or Arg-mediated phosphorylation of catalase on both Y231 and Y386 is necessary for its degradation and thereby control of intracellular oxidant levels

(Figure 4D). The effects of the Y231 and/or Y386 mutations on the tertiary structure of catalase (*19*) may thus provide further insights regarding the regulation of this important effector of redox balance.

Dual Regulation of Catalase by c-Abl/Arg. c-Abl and Arg are activated in response to oxidative stress (*9*, *12*, *13*). Moreover, ROS induce c-Abl−Arg heterodimers, and both c-Abl and Arg are necessary as effectors in the apoptotic response to oxidative stress (*14*). At lower ROS levels, catalase activity is stimulated by c-Abl/Arg-mediated phosphorylation of Y231 and Y386 (*16*) (Figure 4D). In the event that ROS levels continue to increase, c-Abl and Arg dissociate from catalase (*14*), and catalase activity is decreased by (1) tyrosine phosphatases that dephosphorylate Y231-P and/or Y386-P or (2) targeting of phosphorylated catalase for ubiquitination. Proteosomal degradation of ubiquitinated catalase results in increased ROS levels and cell death by apoptosis or necrosis (Figure 4D). The available findings thus support a model in which c-Abl/Arg function in protecting cells from oxidative stress by stimulating catalase activity (*14*) and, in the event of uncontrollable ROS levels, c-Abl/Arg induce catalase degradation and thereby cell death (Figure 4D). These findings provide the first evidence that regulation of the constitutive half-life of catalase by c-Abl and Arg represents a mechanism for controlling catalase levels and redox balance.

REFERENCES

1. Croteau, D., and Bohr, V. (1997) Repair of oxidative damage to nuclear and mitochondrial DNA in mammalian cells, *J. Biol. Chem. 272*, 25409−25412.
2. Berlett, S., and Stadtman, E. (1997) Protein oxidation in aging, disease, and oxidative stress, *J. Biol. Chem. 272*, 20313−20316.
3. Jacobson, M. D. (1996) Reactive oxygen species and programmed cell death, *Trends Biochem. Sci. 21*, 83−86.
4. Manna, S. K., Zhang, H. J., Yan, T., Oberley, L. W., and Aggarwal, B. B. (1998) Overexpression of manganese superoxide dismutase suppresses tumor necrosis factor-induced apoptosis and activation of nuclear transcription factor-kappaB and activated protein-1, *J. Biol. Chem. 273*, 13245−13254.
5. Yin, Y., Terauchi, Y., Solomon, G., Aizawa, S., Rangarajan, P., Yazaki, Y., Kadowaki, T., and Barrett, J. (1998) Involvement of p85 in p53-dependent apoptotic response to oxidative stress, *Nature 391*, 707−710.
6. Migliaccio, E., Giorgio, M., Mele, S., Pelicci, G., Reboldi, P., Pandolfi, P. P., Lanfrancone, L., and Pelicci, P. G. (1999) The p66shc adaptor protein controls oxidative stress response and life span in mammals, *Nature 402*, 309−313.
7. Kruh, G. D., Perego, R., Miki, T., and Aaronson, S. A. (1990) The complete coding sequence of arg defines the Abelson subfamily of cytoplasmic tyrosine kinases, *Proc. Natl. Acad. Sci. U.S.A. 87*, 5802−5806.
8. Kharbanda, S., Ren, R., Pandey, P., Shafman, T. D., Feller, S. M., Weichselbaum, R. R., and Kufe, D. W. (1995) Activation of the c-Abl tyrosine kinase in the stress response to DNA-damaging agents, *Nature 376*, 785−788.
9. Sun, X., Wu, F., Datta, R., Kharbanda, S., and Kufe, D. (2000) Interaction between protein kinase C δ and the c-Abl tyrosine kinase in the cellular response to oxidative stress, *J. Biol. Chem. 275*, 7470−7473.
10. Cao, C., Ren, X., Kharbanda, S., Koleske, A. J., Prasad, K., and Kufe, D. (2001) c-Abl-related Arg interacts with SIVA in the apoptotic response to oxidative stress, *J. Biol. Chem. 276*, 11465−11468.
11. Ito, Y., Pandey, P., Mishra, N., Kumar, S., Narula, N., Kharbanda, S., Saxena, S., and Kufe, D. (2001) Targeting of the c-Abl tyrosine kinase to mitochondria in endoplasmic reticulum stress-induced apoptosis, *Mol. Cell. Biol. 21*, 6233−6242.
12. Sun, X., Majumder, P., Shioya, H., Wu, F., Kumar, S., Weichselbaum, R., Kharbanda, S., and Kufe, D. (2000) Activation of the cytoplasmic c-Abl tyrosine kinase by reactive oxygen species, *J. Biol. Chem. 275*, 17237−17240.
13. Kumar, S., Bharti, A., Mishra, N., Kharbanda, S., Saxena, S., and Kufe, D. (2001) Targeting of the c-Abl tyrosine kinase to mitochondria in the necrotic cell death response to oxidative stress, *J. Biol. Chem. 276*, 17281−17285.
14. Cao, C., Leng, Y., and Kufe, D. (2003) Functional interaction between the c-Abl and Arg protein tyrosine kinases in the oxidative stress response, *J. Biol. Chem. 278*, 12961−12967.
15. Amstad, P., Peskin, A., Shah, G., Mirault, M. E., Moret, R., Zbinden, I., and Cerutti, P. (1991) The balance between Cu,Zn-superoxide dismutase and catalase affects the sensitivity of mouse epidermal cells to oxidative stress, *Biochemistry 30*, 9305−9313.
16. Cao, C., Leng, Y., and Kufe, D. (2003) Catalase activity is regulated by c-Abl and Arg in the oxidative stress response, *J. Biol. Chem. 278*, 29667−29675.
17. Koleske, A. J., Gifford, A. M., Scott, M. L., Nee, M., Bronson, R. T., Miczek, K. A., and Baltimore, D. (1998) Essential roles for the Abl and Arg tyrosine kinases in neurulation, *Neuron 21*, 1259−1272.
18. Fridovich, I. (1997) Superoxide anion radical (O_2), superoxide dismutases, and related matters, *J. Biol. Chem. 272*, 18515−18517.
19. Putnam, C. D., Arvai, A. S., Bourne, Y., and Tainer, J. A. (2000) Active and inhibited human catalase structures: ligand and NADPH binding and catalytic mechanism, *J. Mol. Biol. 296*, 295−309.

BI035023F